ISSN(PRINT) : 2320 -1967
ISSN(ONLINE) : 2320 -1975

GLOBAL SCIENTIFIC INC.

ChemXpress

ORIGINAL ARTICLE

CHEMXPRESS 4(4), 312-324, (2014)

Study of the protective properties of organic coatings for encapsulation of photovoltaic cells

V.Marzocchi[1], C.R.Tomachuk[2], A.R.Di Sarli*[3], F.Bellucci[1]

[1]Dipartimento di Ingegneria dei Materiali e della Produzione, Università degli Studi di Napoli "Federico II", P.le Tecchio, 80, 80125, Napoli, (ITALY)
[2]Engineering School of Lorena of the University of San Pablo (EEL-USP), Environment and Basic Sciences Department, Estrada do Campinho s/n, CEP 12602-810, Lorena, SP, (BRAZIL)
[3]CIDEPINT: Research and Development Centre in Paint Technology (CICPBA-CONICET La Plata); Av. 52 s/n entre 121 y 122. CP. B1900AYB, La Plata, (ARGENTINA)
E-mail: ardisarli@cidepint.gov.ar; bellucci@unina.it; celiatomachuk@usp.br
Received : 18th October, 2013 ; Revised : 23rd December, 2013 ; Accepted : 03rd January, 2014

Abstract : The protective properties of encapsulating materials such as organic coatings deposited on simplified photovoltaic cells modules (glass/ZnO/encapsulating material) and subjected to 0.6 M NaCl solution were investigated. The organic coatings lifetime is related to the reactants diffusion into the bulk and to the adhesion at the ZnO/encapsulating material interface. EIS measurements were used to investigate the corrosion phenomena at the ZnO/encapsulating interface. Capacitance Fast Transient Technique (CFTT) was utilized to evaluate water uptake and the barrier properties of the polymeric films, while DSC measurements and SEM micrographs were employed for samples' characterization. According to the EIS data obtained and analyzed along the tests in neutral chloride solution, the protective performance afforded by the Ionomeric coating (polyethylene-acrylic acid copolymer including ionic species) was much more effective than the corresponding to the EVA (ethyl vinyl acetate copolymer) and PU (polyurethane) coatings.

Keywords : PV encapsulation; Photovoltaic module; EIS; CFTT; Thin film.

INTRODUCTION

Degradation of polymeric coating materials has been investigated for many years. Environmental factors, such as light, oxygen, moisture, salts, acids, temperature are critical factors for coating degradation[1], therefore, new products are created and the main material properties are modified.

The thermal stability of polymer materials determines their durability and the environment where can be applied. In practice, the functional parameters, especially lifetime, deteriorate according to the extent of ageing.

A critical component of a photovoltaic (PV) mod-

ule is the encapsulation material that provides structural support, optical coupling, electrical isolation, physical isolation/protection, and thermal conduction for the solar cell assembly[2].

Taking into account that the thin zinc oxide films have many applications, the protective properties of some encapsulating materials applied on thin ZnO films utilized in photovoltaic modules were investigated. With this purpose, the ZnO was deposited on ceramic substrates giving as result metal films with high adhesive strength even on smooth substrates[3]. It should be denoted that due to its high optical transparency, materials make of this mode are also used as front contact (transparent conductor) in solar cells[4]. In this case, the light radiation coming from the ZnO side reaches the $CuInSe_2$, where the charges photo-generation takes place. The thus produced holes and electrons migrate respectively towards the zinc oxide and molybdenum where they could be used in the external load[5-7].

Figure 1 shows a simplified diagram of how work a thin film photovoltaic cell called CIS module.

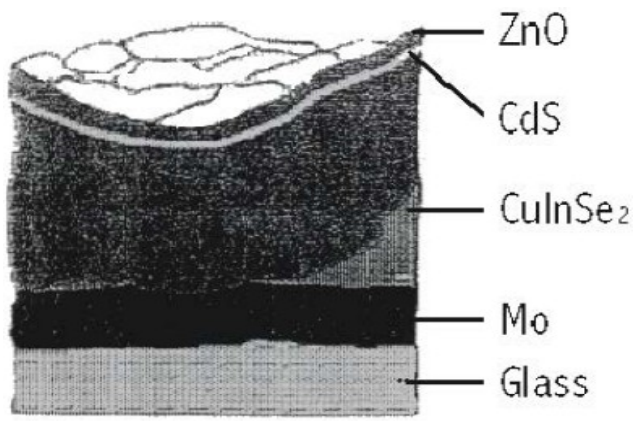

Figure 1 : Example of CIS module

The photovoltaic cells are prepared by chemical vapor deposition (CVD) on glass substrates. During its exposure to aggressive environment, and once reached by the penetrating agents, especially water, the first layer that degrades is the zinc oxide film, which undergoes a significant increase in its resistivity.

In full daylight solar cells work at temperatures between 70 °C and 90 °C, but during the night these last can reach values less than 0 °C, even up to -40 °C in space applications. As a consequence of these changes, the photovoltaic cells are subjected to thermal cycles of high amplitude, which make that the materials be affected by extremely severe mechanical strains. Therefore, the thermal stress plays a major role in the photovoltaic modules degradation and, in this regard, the IEC 1646 standard for testing the aging of solar cells to be used in professional installations establish that those must be tested using thermal cycles of -40 °C to +85 ºC. On the other hand, the moisture and ionic impurities (salts, dust, etc.) represent some of the main enemies of cell photovoltaic modules. The presence of an electrolyte solution could lead to the cell photoactive layer (ZnO) and/or electrical contacts corrosion.

Furthermore, the combined action of water and temperature can promote the coating delamination and, with this, promoting a faster contact substrate/penetrating materials underneath the outer coating. As a result of all these events, the ZnO aging affects the semiconductors properties, reason by which it is necessary isolate it from the environment. This can made encapsulating the module with inert materials. The protective coating should provide a barrier against external agents as well as resistance to mechanical stresses. Besides, the encapsulating material must[8]:

- to contain only solvent not harmful to the photoactive layer;
- to provide an effective barrier against water, oxygen and ionic species;
- to be stable against the sunlight;
- to be transparent to solar radiation of wavelengths between 400 and 1100 nm to allow the light reaches the photoactive layer;
- to be resistant to thermal fatigue;
- to have mechanical strength and surface hardness;
- to have good adhesion properties with the substrate;
- to ensure the electrical isolation of the PV module, limiting the leakage current to the outside.

The barrier effect offered by an organic coating is a key factor in the anticorrosive protection provided to the substrate since the water, oxygen and aggressive ions are the species responsible for the onset of the corrosion process[9]. Hence, the coating degradation evolution has been monitored by measuring the coated system impedance because many authors reported that changes of the resistive and capacitive components of such impedance during the immersion in chloride solution[10] were attributable to the coating degradation[11].

ORIGINAL ARTICLE

The thermal stability of polymer materials determines their durability and the environment where they can be applied. In practice, the functional parameters, especially life time, deteriorate according to the extent of ageing.

As some polymeric materials are able of solving the encapsulation system, the aim of the present work was to study how the barrier properties and water absorbed by the organic coating are related to the degradation process of the underlying photovoltaic modules. The polymeric coating behavior has been investigated by electrochemical impedance spectroscopy (EIS), because it allows obtaining information about properties of the coating system such as the presence pores and/or other defects, adhesion, etc. In this sense, it is evident that for obtaining these results is necessary to distinguish the contribution of the different system' components to the overall impedance values measured as a function of the frequency, therefore, to found an equivalent electrical circuits model that can fit adequately the impedance spectra[12].

Electrochemical techniques were utilized to monitor the degradation of both the polymeric encapsulating and the photoconductive substrate during the exposure time to the aggressive environment. Electrochemical Impedance Spectroscopy (EIS) measurements were used to investigate the corrosion phenomena at the ZnO/encapsulating interface and the obtained data were fitted by using an equivalent circuit developed to simulate the organic coating surface degradation. Capacitance Fast Transient Technique (CFTT) was used to evaluate the water uptake and barrier properties of the polymeric films, while DSC measurements and SEM micrographs were employed for samples' characterization. The exposure medium was an aerated 0.6 M NaCl solution at 25 °C or 80 °C.

In this work, three encapsulating materials for photovoltaic (PV) modules, namely, EVA (ethyl vinyl acetate copolymer), PU (polyurethane) and Ionomer (polyethylene acrylic acid copolymer without and with Na^+ and Zn^{2+} as ionic species) were investigated.

Ethylene vinyl acetate (EVA) copolymer has several applications, such as corrosion protection, electrical insulation, scratch films, hoses and manufacture of adhesives, including hot melts[13]. Various formulations containing vinyl acetate in polyethylene matrix are susceptible to changes in their crystallinity as other physical and chemical features[14-17]. For PV applications, the content of the vinyl acetate is about 33% wt[8].

Allen et al.[16] investigated the thermal oxidation, stabilizations and yellowing by thermo-gravimetric and hydroperoxide analysis, FTIR, fluorescence spectroscopy and yellowness index of ethylene-vinyl acetate copolymer (EVA-17 and 28% wt vinyl acetate units). The results show that the main degradation routes for EVA involve the initial loss of acetic acid followed by oxidation and breakdown of the main chain, confirming date of the McNeil et al.[18]. The degradation rate is greater in an oxygen atmosphere as is the formation of cured products. Hydroperoxidation is an important route in the oxidation and yellowing of EVA copolymers giving rise to ketone and unsaturated ketone groups.

The performance reliability of the EVA copolymer encapsulants used for photovoltaic modules was studied by Pern and Czanderna[8,19,20]. They have observed delamination of the EVA encapsulated solar cells from glass superstrates or Tedlar™ substrates and blistering of the Tedlar™ backing film due to gaseous organic products accumulated from EVA degradation. Pern[19] showed that UV-induced EVA browning in solar cells at 85±2 °C is much greater than from simple heating at the same temperature. The EVA discoloration rate can be affected by chemical and physical factors. The chemical factors include the: (a) EVA formulation and additive used; (b) presence and concentration of curing-generated; UV-excitable chromophores that depend on the type of curing agent used; (c) loss rate of the UV absorber; (d) curing agent and curing conditions; and (e) photo bleaching reactions of chromophores resulted from diffusion of air (oxygen) into the laminated films. The physical factors include the: (a) UV light intensity; (b) UV-filtering effect of glass superstrates; (c) gas permeability of polymeric superstrates; (d) lamination-delamination; and (e) laminated film thickness[19].

The transport of water and gases (oxygen and carbon dioxide) through EVA films of different VA content were analyzed by permeation measurements proposed by Marais et al. The results will indicate that the increase in water sorption extent with the VA content leads to a steady increase in the water permeability in the EVA copolymers. Gas permeation, both O_2 and CO_2 and whatever the VA content of the copolymers used,

ORIGINAL ARTICLE

was characterized by a constant diffusion coefficient.

Polyurethane (PU) is now being increasingly used for the surface protection of materials like materials like metals, plastics, wood, glass fibers, as well as in the microelectronics industries[21]. Photo-oxidative degradation and yellowing/discoloration in polymers/coatings upon UV irradiation are a common phenomenon[22-25]. Therefore, it is important to study its corrosion resistance in aggressive environments and it has not been studied in detail.

The photodegradation process of polyurethane coatings was investigated to Zhang et al.[24] by positron annihilation spectroscopy and a direct correlation with cross-link density was observed. The correlation was interpreted in terms of a classic photodegradation mechanism involving radical formation after breaking chemical bonds, formation of new cross-links and loss free-volume. This process will eventually lead to failure of the protective function of polymeric coatings or loss of coating durability.

Pulat et al.[26] investigated the structural and surface properties of polyurethane membranes of different porosities prepared by a classical solvent-casting method. The results shows that water permeability of the polyurethane increases as the porosity increase and can be compared to the water permeability of some commercial membranes used in wound healing.

Ionomer can be defined as macromolecules (polymer) containing a small percentage of ionic groups (typically less than 10% mol) chemically bound and distributed in non-ionic backbone chains and it has been investigated by many research group with a great deal of interest[27]. From the academic and industrial point of view, the relationship between the chemical structure, the morphology and the physical properties of the Ionomer is of primary interest. The modulus, glass transition temperature, viscosity, melt strength, fatigue, transport and many other properties can be influenced by ion incorporation onto to polymer. Thus, Ionomer are technically important polymers with many commercial applications and its properties have been extensively studied[28-30].

MATERIALS AND METHODS

Samples preparation

On soda-lime glass substrates of 10 x 10 cm provided by Zentrum für Sonnenenergie und Wasserstoff-Forschung –ZSW, Stuttgart, Germany, the thin ZnO films were deposited by PVD technique using DC-magnetron sputtering equipment operating under proprietary conditions. Then, these samples were covered with any of the following encapsulating materials: EVA (ethyl vinyl acetate copolymer); PU (polyurethane); Ionomer A or Ionomer B with a base of polyethylene-acrylic acid copolymer including ionic species of patented composition, TABLE 1. The thickness and composition of the tested samples are also reported in this TABLE.

TABLE 1 : Specification and thickness of the samples furnished by ZSW

Samples	Composition	Thickness (μm)	
		ZnO	Organic coating
S1	ZnO + EVA (ethylvinylacetate copolymer with 33% vinyl acetate)	0.5	200
S2	ZnO + PU (polyurethane)	0.5	400
S3	ZnO + IonomerA (polyethylene-acrylic acid copolymer)	0.5	300
S4	ZnO + IonomerB (polyethylene-acrylic acid copolymer including Na^+ and Zn^{2+} as ionic species)	0.5	230

Thickness measurements

Coatings thickness was measured by the Helmut Fischer equipment DUALSCOPE MP4.

Electrochemical behavior

A systematic study of the corrosion behavior of the ZnO/encapsulation materials in aqueous aerated chloride solution was carried out by Electrochemical Impedance Spectroscopy (EIS) and Capacitance Fast Transient Techniques (CFTT). The accelerated immersion tests took place in aerated 0.6 M NaCl solution, pH 7, at 25 °C or 80 °C.

In all cases, the three electrodes electrochemical cell was made by sealing a glass cylinder onto each sample (working electrode) by an O-ring, which left an exposed sample surface area of 3.14 cm^2; the

ORIGINAL ARTICLE

reference and counter electrodes were respectively one of Ag/AgCl and a platinum mesh. Throughout this paper, all the electrochemical potential values are referenced with regard to the Saturated Calomel Electrode (SCE).

EIS measurements were performed in the frequency range between 10^{-2} – 10^{5} Hz using a Solartron 1255 Frequency Response Analyzer (FRA) coupled to a Solartron 1296 dielectric interface, and a sinusoidal voltage signal of 50 mV. The experimental spectra were interpreted on the basis of equivalent electrical circuit models obtained from the ZView fitting software developed by Scribner Associates®.

The CFTT measurements based upon the coating capacitance evolution determined from the Brasher–Kingsbury[31] equation is the most direct way to estimate the amount of water contained within an organic coating:

$$\phi = \frac{\log(C_t / C_0)}{\log(\varepsilon_w)} \quad (1)$$

where, C_t is the coating capacitance at the time t, C_0 the "dry" coating capacitance, and ε_w the water uptake dielectric constant.

The diffusion coefficient was calculated using the following equation:

$$D = \frac{1}{4} L^2 \Psi^2 \pi \quad (2)$$

where, L is the organic film thickness and Ψ is the slope of the linear part of the curve

$$\mathrm{Ln}\frac{C}{C_\infty} \text{ vs. } \sqrt{t} \quad (3)$$

where C is the coating capacitance or water mass uptake at time (t) and C_∞ is the coating capacitance in condition of water saturation.

The CFTT measurements were carried out at a frequency of 10^4 Hz for 16 hours using an electrochemical interface Solartron 1287.

All the measurements were performed at laboratory temperature (24±2 ºC), and with the electrochemical cell inside a Faraday cage to reduce external interferences as much as possible.

Morphology

The samples morphology was characterized by SEM images using a LEICA S440 microscope.

Differential scanning calorimeter measurements

The Differential Scanning Calorimeter (DSC) analysis was performed with a Mettler-TA89A equipment operating in nitrogen atmosphere at a heating rate of 10 °C/min. Two-step swept from 20 °C to 200 °C at constant rate was performed to obtain information about the samples' thermal properties. Open-top aluminum crucibles together with an empty crucible as reference were used in each test.

The sampling involved to remove small amounts (≈ 10 mg) of the polymeric film with a scalpel, place them in the crucible, which was sealed tight and analyzed.

In order to improve the experimental data reliability, three replicates of each specimen were measured after characterizing their surface parameters.

RESULTS AND DISCUSSION

Electrochemical behavior

(a) EIS measurements

TABLE 1 reports the identification symbol, chemical composition and overall coating thickness of the samples prior to exposure. It was possible to observe that they were uniform and bright throughout the entire surface. As can be seen, all the samples had similar and uniform thickness throughout the entire surface.

A qualitative description of the coating protective properties was obtained by electrochemical impedance spectroscopy measurements performed at room (25 °C) or high (80 °C) temperature.

Figure 2a shows the impedance module values of samples tested at the initial and after 90 days of immersion in 0.6 M NaCl solution at T = 25 °C. As can be seen, only the S2 impedance values decreased significantly after 90 days immersion. However, the part b) of this figure illustrating the phase angle evolution demonstrates that the corresponding to S1 and S4 samples evidenced the presence of more than one time constant from the first immersion day, while it was seen after 90 days for S4 samples and not at all for S3 samples. This suggests that in S1, S2 and S4 samples the solution arrived to the polymer/ZnO allowing the development of hydroxides of the metal according to the following general reaction:

$$ZnO + H_2O \longrightarrow ZnO(OH)_2$$

Figure 3a-b shows respectively the impedance module and phase angle values of samples tested at the initial and after 90 days of immersion in 0.6 M NaCl solution at T=80 °C. By analyzing the impedance spectra plotted in this figure is easy of seen that the degradation processes observed in S1, S2 and S3 samples at 25 ºC were strongly accelerated by increasing the exposure temperature. Again, the S4 samples response did not show any change visible by naked eye.

(b) Modeling the degradation process

A quantitative interpretation of the impedance spectra evolution was conducted by fitting the 100% of data obtained from each individual test and accepting a maximum error ≤ 5%.

After many attempts to find the better equivalent circuit capable of simulate the experimental impedance data it was assumed that the most probable one was the shown in Figure 4. In it, C_{coat} and R_{coat} correspond respectively to the coating capacitance and resistance, while C_{dl} (electrochemical double layer capacitance) and R_{ct} (charge transfer resistance) were associated to the corrosion process.

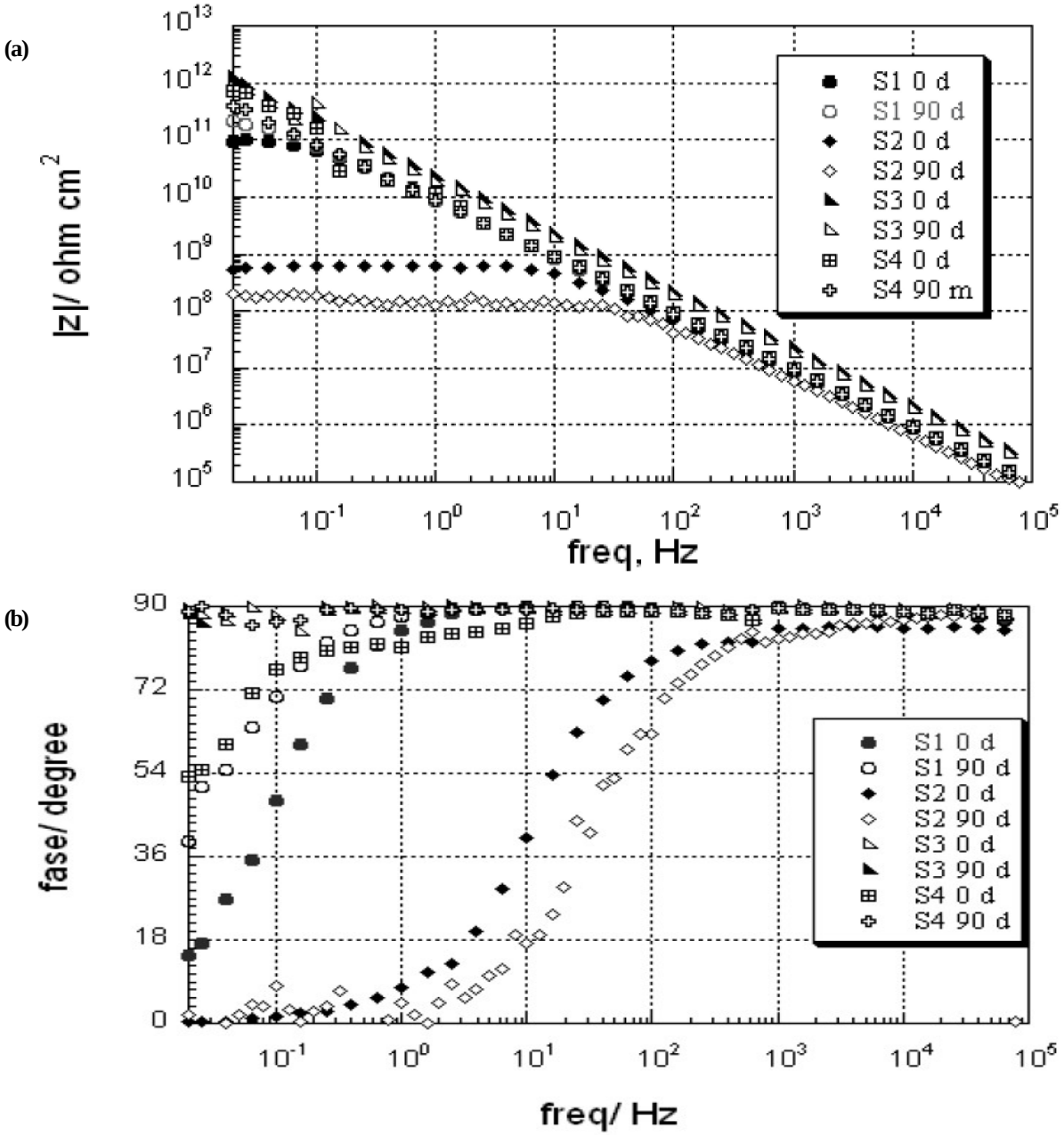

Figure 2 : EIS measurements (a) samples impedance module and (b) phase angle at 25 °C.

ORIGINAL ARTICLE

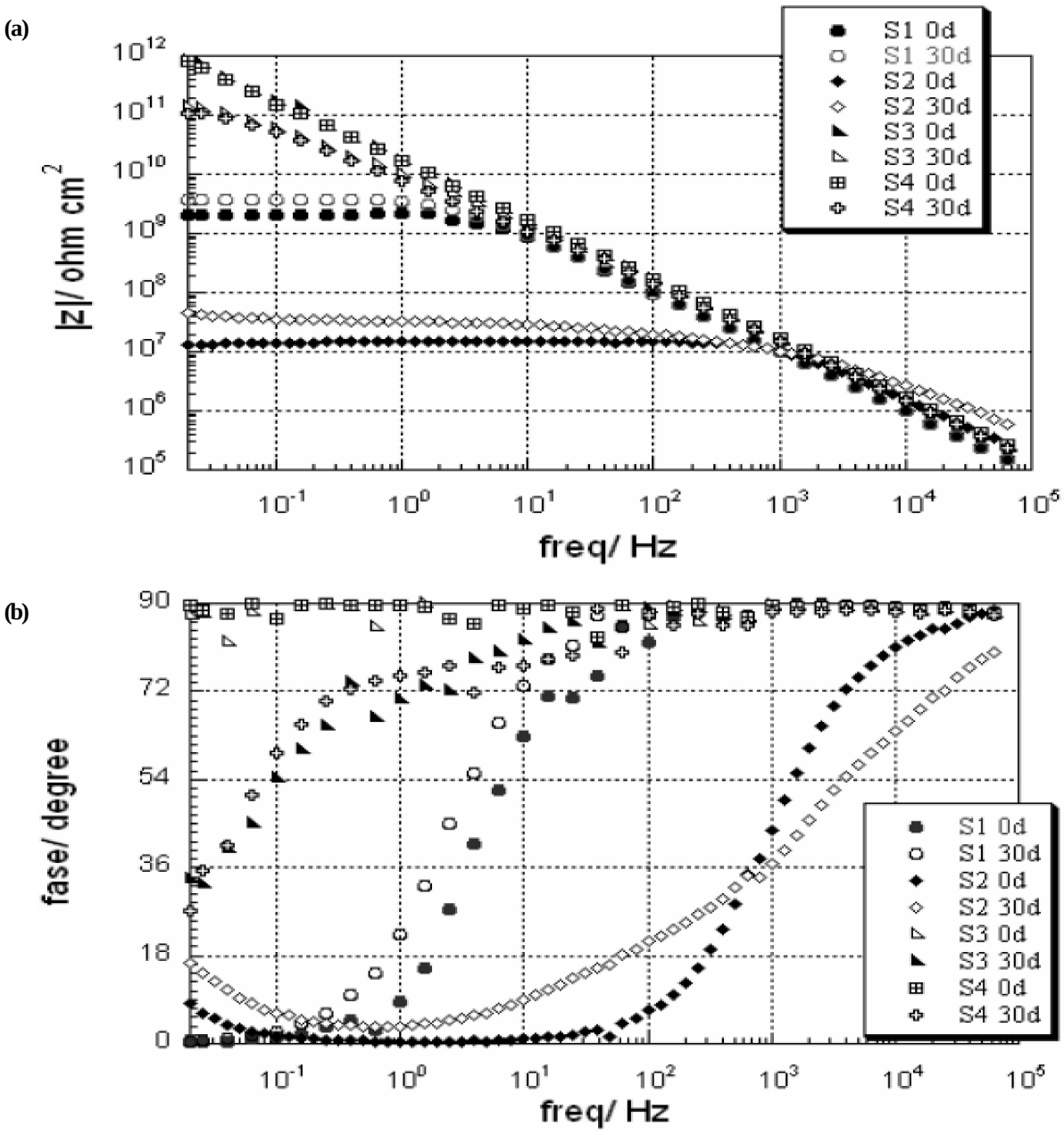

Figure 3 : EIS measurements (a) samples impedance module and (b) phase angle at 80 °C.

The results at 25 °C were mostly modeled with an equivalent electrical circuit only formed by the coating resistance (R_{coat}) in parallel with a CPE (constant phase elements), which replaced the C_{coat} as component of the described circuit.

Figure 5a illustrates the coatings (CPE_{coat}, R_{coat}) parameters evolution at 25 ºC for the tested samples. In this Figure is important to remark the absence of R_{coat} values corresponding to S3 samples; such a result could be explained assuming that being the phase angle value almost constant and ≈ 90º (see Figure 2b) in the entire frequency range swept, the coating always behaved as an impervious dielectric, avoiding as a consequence the occurrence of other physicochemical processes (diffusion of water and chemicals, corrosion reactions, etc.) within a so complex interface. Besides, this means not only that in the impedance data fitting the CPE must be replaced by a capacitor but also that the R_{coat} magnitude tends to "infinite". The other three coatings also showed a very high and continuous protective capacity with R_{coat} values greater than 10^8 Ω.cm^2 and C_{coat} less than 10^{-10} F.cm^{-2} throughout the entire test. As a gen-

eral rule, these resistance and capacitance values are characteristic of less deteriorated organic coatings[31]. Besides, this means that the amount of water uptake in each case could be less than 5% of the painting system volume[32] over the test.

Figure 5b shows that the coatings degradation processes were more evident by increasing the temperature up to 80 ºC; particularly in the case of S3 samples where such degradation was evidenced by the R_{coat} decrease from 10^{13} Ω.cm^2 to ≈ $10^{8.8}$ Ω.cm^2 before 100 h exposure. With regard to S1 and S2 samples, their coating resistance was about one order the magnitude less than the obtained at 25 ºC, while the coupled capacitance values remained very similar in the range 10^{-10}-10^{-11} F.cm^{-2}. The strongly lower R_{coat} values obtained at 80 ºC than those at 25 ºC for S3 and S4 samples did that the test of both types was given by ended after 700 h exposure. To explain this shorter protective performance was presumed that the high temperature of the electrolyte medium turned it very aggressive towards the organic coating structure, provoking the accelerated breakup of the polyethylene-acrylic copolymer forming part of the Ionomeric coating formulations.

CFTT measurements

CFTT measurements were carried out to evaluate the water uptake and its diffusion coefficient within the tested organic coatings.

In agreement with the most recognized model for evaluating the water uptake trend in organic coatings, i.e. monitoring of the coating capacitance variation as a function of the exposure time square root ($\sqrt{t}$), it is pos-

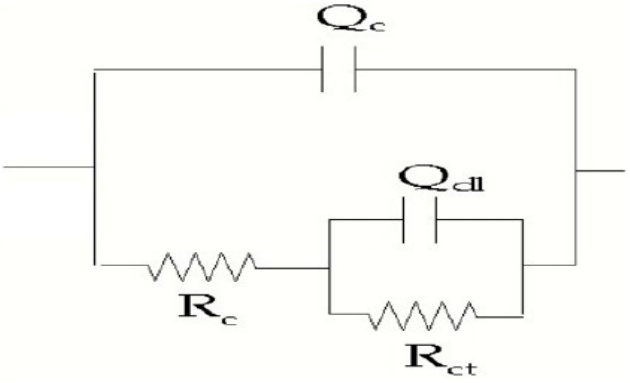

Figure 4 : Equivalent circuit.

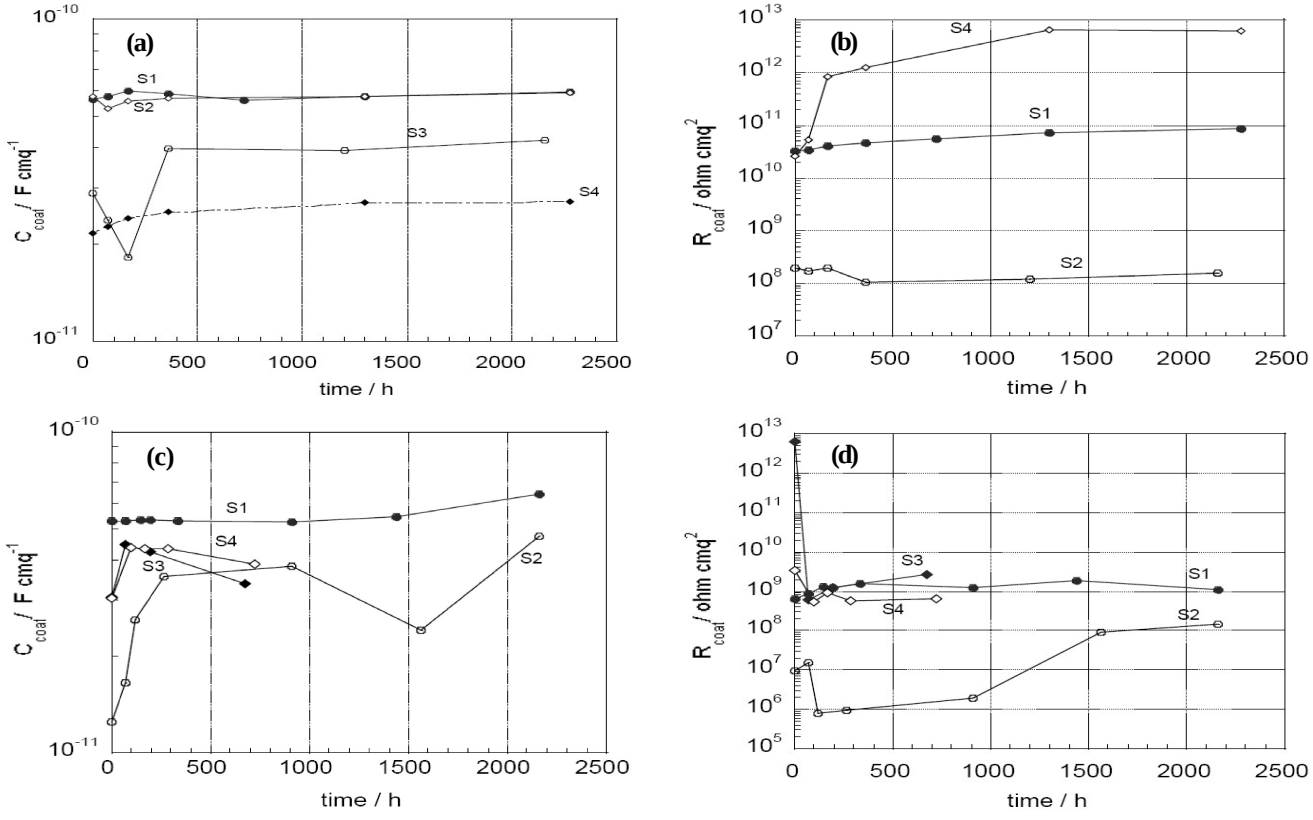

Figure 5 : Evolution of C_{coat} and R_{coat} parameters corresponding to S1, S2, S3 and S4 samples immersed in 0.6 M NaCl solution at a) T= 25 ºC or b) 80 ºC.

ORIGINAL ARTICLE

sible to observe three distinct regions which are schematically reported in Figure 6. Initially, there is a homogeneous water diffusion within the dry coating - region I; the fast increase of the film capacitance at short immersion times is generally associated to the water permeation within the coating, which fill up the intrinsic coating free volume, and to the fact that the water dielectric constant ($\varepsilon_w \approx$ 78-80 F.cm^{-1} at 25 ºC) is much greater than the corresponding to the organic coating ($\varepsilon_c \approx$ 4-8 Fcm^{-1}). At the end of this first step, the polymeric matrix saturates and its capacitance value remains stable - region II. Finally, a further increase in the coating capacitance value is attributed to the coating swelling and/or the water accumulation at the coating/substrate interface - region III.

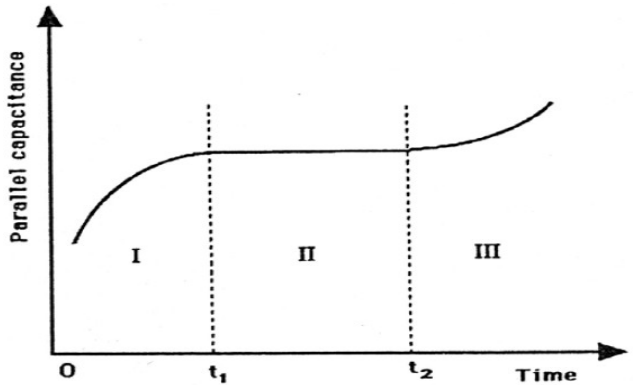

Figure 6 : Schematic plot of the organic coating capacitance evolution as a function of the exposure time to an aqueous electrolyte.

Figure 7a show capacitance transient for S1 sample (ZnO+EVA) for 16 hours of immersion in neutral 0.6 M NaCl solution at 25 ºC (Figure 7a) and 80 °C (Figure 7b), respectively. Data obtained at 25 °C obey a typical Fickian behavior up to the free volume within the coating film was saturated with the permeated water. The presence of a second linear region can be attributed to the presence of a bi-layer coating structure. A deeper analysis related to the transport properties of these layers suggest a structure made of an outer porous and inner compact layer. This complex coating structure could be attributed to the processing adopted. It must be mentioned that for 16 hours of immersion in the test solution, the phase angle value remained stable at approximately 89.4º, suggesting a homogeneous water distribution within the coating.

As shown in Figure 7b, quite different was the absorption behavior at 80 °C. The initial lineal rise of capacitance fatly disappears being replaced by a decrease of the same as the time elapsed. The phase angle values, however, did not differ from that observed at 25 °C. The different water absorption kinetic at high temperature could be interpreted assuming that the water diffusion rate increased in such a manner that the water permeability of the coating film is so high that its dielectric behavior does not comply with the assumptions made to solve the calculation model[33], i.e., with the Fick' laws related to the mass transport. In addition, the water uptake could provoke the swelling of the coating and, consequently, an increase of the film effective thickness, variable this indirectly correlated to the coating capacitance values.

Figure 7c) and d) show the transients of the coating capacitance for S2 samples (ZnO+PU) immersed in 0.6 M NaCl solution at 25 ºC or 80 ºC, respectively. In both plots, an increase of the capacitance values as a function of the exposure time can be seen; on the other hand, such increases were simultaneously accompanied by a decreased of the phase angle values from 87º to 80º. The continuous coating capacitance increment associated to a decreasing phase angle suggested that the presence of water molecules clusters lead to decrease the diffusion coefficient value but to increase the number of conducting pathways of lower resistance to the electrolyte diffusion short-circuiting the organic coating film[34].

Figure 7e) shows that data obtained for S3 samples (ZnO+IonomerA) at 25 ºC also obey a typical Fickian behavior up to the free volume within the coating film was saturated with the permeated water, after this, a more or less defined plateau was observed. On the other hand, the part f) of this figure allows seeing that at 80 °C the coating capacitance did not change significantly.

This result suggests a simple Fickian behavior as far as the transport of water is concerned. The constant phase angle 90 e 89 respectively supports a Fickian kinetic of water sorption into the polymeric matrix.

Figure 7g) and h) show the transients of the coating capacitance for S4 samples ((ZnO+IonomerB) during 16 hours of immersion in 0.6 M NaCl solution at 25 ºC or 80 ºC, respectively. The appearance of a first plateau at C ~ 17.2 pFcm^{-2} at about 15 minutes of immer-

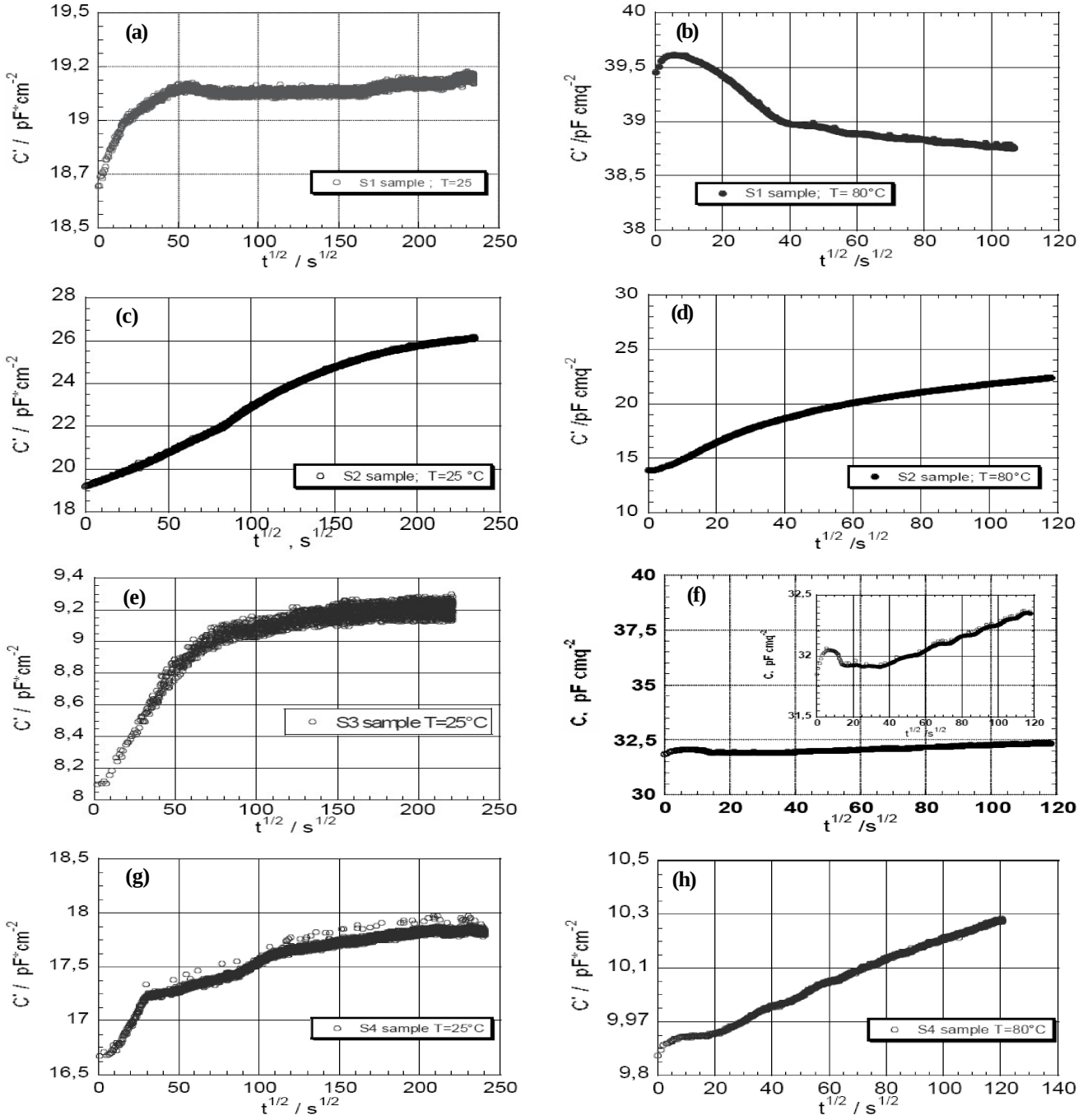

Figure 7 : Evolution of S1, S2, S3 and S4 samples capacitance as a function of √t during immersion in 0.6 M NaCl solution at a) 25 ºC or b) 80 ºC.

sion, observed at 25 ºC (Figure 7g), indicates that the coating is reaching its water saturation value. Suddenly, a new increase of the slope of the capacitance curve indicates the starting of new phenomena supposed to involve formation corrosion products in the coating/ZnO interface. This behavior suggests that ionic species (Na^+ and Zn^{2+} added in copolymer) does not improve its adhesion properties. After 3 hours of immersion a sharp increase of capacitance was observed which could be attributed to water condensation in voids or the coating metallic interface. In this case, a small percentage of water acts as a plasticizer and causes swelling of the polymer structure which makes it possible that water molecules enter intermolecular voids that were too small before this swelling occurred. On the other hand, the part h) is similar Figure 7f and the same considerations apply.

ORIGINAL ARTICLE

Morphology behavior

(a) DSC measurements curves

Figure 8a-b shows the experimental results of the DSC technique applied on the thermoplastic samples. As seen in Figure 8a, the peak detected at 51 ºC during the first heating of S1 sample appeared less significant and displaced at 61 ºC during the 2nd one, in both cases, such peaks were attributed to the solvent evaporation. The S2 sample response exhibited no peak but further a rubbery conduct. On the other hand, the S3 and S4 samples (Figure 8b), without any solvent added to its coating formulation, presented a qualitatively similar evolution as a function of the temperature and a well-defined peak at 100 °C which could be attributed to the fusion coating.

(b) SEM morphologies

Figure 9 shows the surface images obtained by SEM of the: a) "as-received"; and (b, c and d) after electrochemically treated samples. Samples that are not listed showed no particular characteristics.

After exposed to the NaCl solution at T = 80 °C, and performed the EIS measurements, the original "tissue form" structure of S2 sample (Figure 9a) changed to a surface covered with bubbles (Figure 9b).

On the other hand, after the same exposure conditions, the CFTT measurements carried out in S1 sample

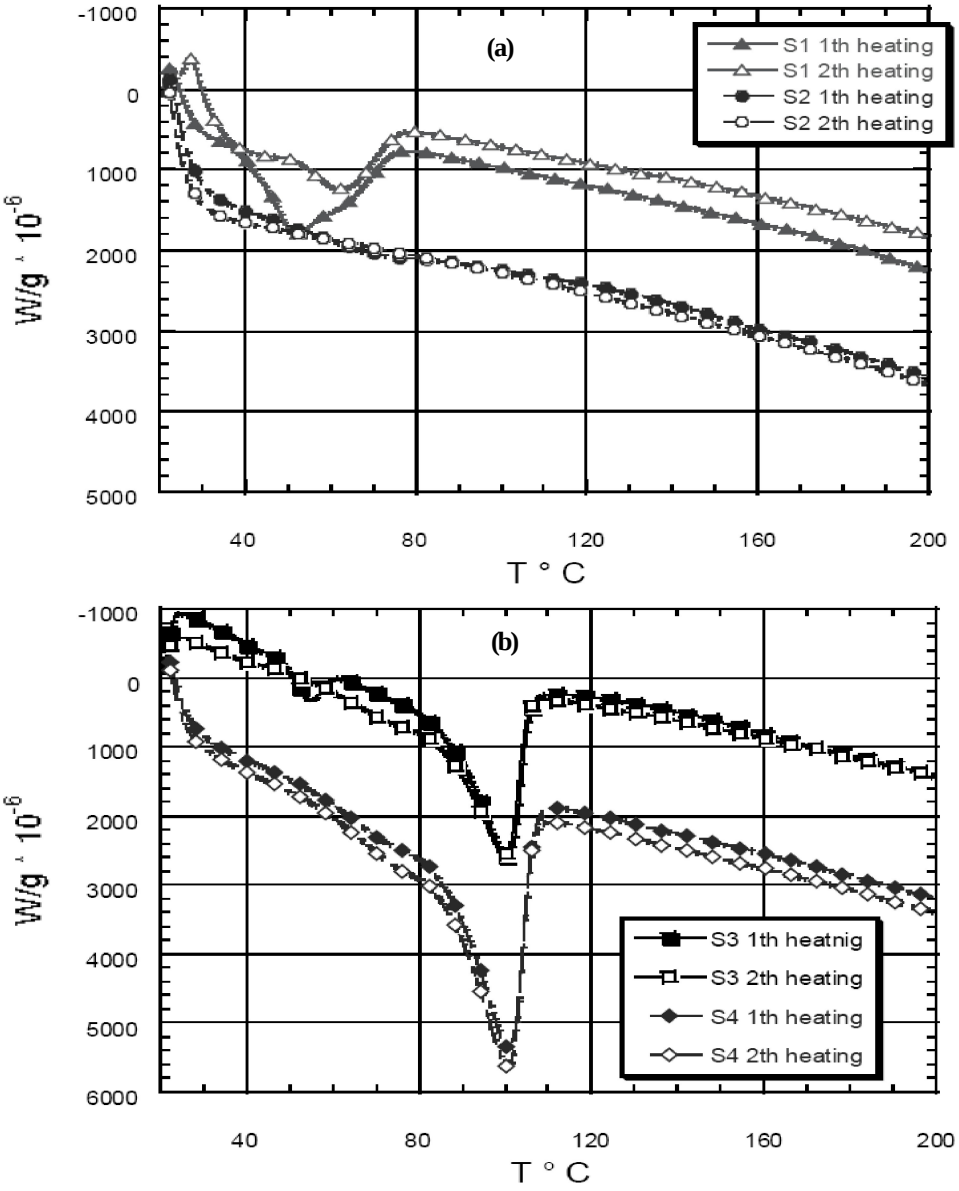

Figure 8 : DSC measurements.

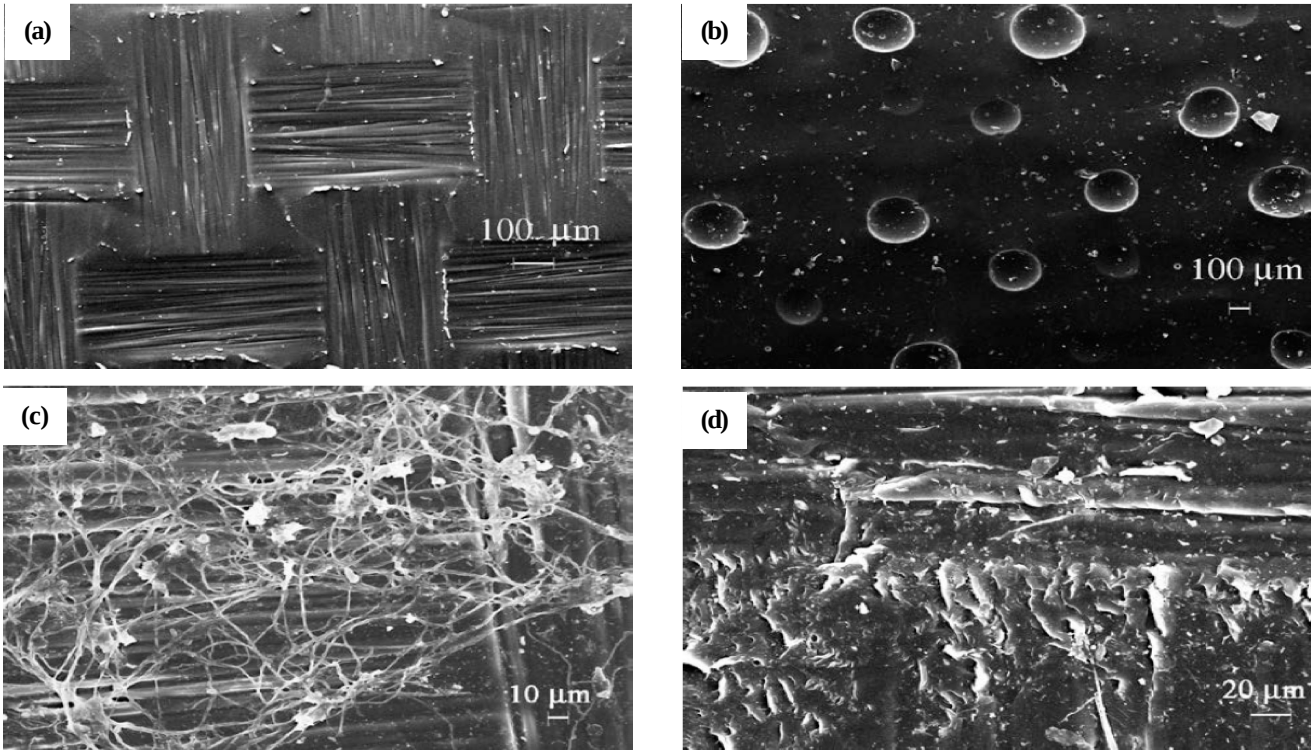

Figure 9 : Coatings surface morphology: (a) "as received"; (b) S2 sample after EIS measurement at 80 °C; (c) S1 and (d) S3 samples after CFTT measurements at 80 °C.

(Figure 9c) show a clear break of the fibber, result clearly in agreement with the high capacitance values illustrating the Figure 7b. Finally, the Figure 9d confirms the fibber degradation of S4 sample, demonstrated by its capacitance evolution (Figure 7h), this result was quite similar to the obtained but not reported when the S3 sample was tested.

CONCLUSIONS

From the results generated during the investigation of the protective properties of encapsulating materials such as organic coatings deposited on simplified photovoltaic cells (glass/ZnO/encapsulating material) and subjected to 0.6 M NaCl solution at 25 ºC or 80 ºC, the following conclusions can be made:

- the protective properties of the tested polymeric films exhibited a remarkable dependence on the exposure temperature, which significantly accelerate the global coating degradation;
- at the higher testing temperature (80 °C), all the organic coatings properties changed making possible easier water permeation. As a consequence, the degradation of both the coating protective as well as the zinc oxide electrical properties started sooner;
- based on the resistivity values exhibited by each sample at 80 °C, the following ranking of the system performance can be established: ZnO/Ionomer > ZnO/EVA > ZnO/PU samples;
- the electrochemical best performance was offered by the both Ionomer (ZnO/IonomerA and ZnO/IonomerB) followed by ZnO/EVA sample;
- the ZnO+PU sample exhibited the fastest degradation rate.
- CFTT technique provided useful information on the kinetic of water diffusion within the organic coating.

ACKNOWLEDGEMENTS

The Comisión de Investigaciones Científicas de la Provincia de Buenos Aires (CICPBA) and the Consejo Nacional de Investigaciones Científicas y Técnicas (CONICET) of Argentina

REFERENCES

[1] S.M.Hamid; Handbook of Polymer Degradation, 2nd Revised and Expanded Edition, New York, Marcel Dekker, **(2000)**.

ORIGINAL ARTICLE

[2] C.Brabec; Solar Energy Materials and Solar Cells, **83**, 273 **(2004)**.

[3] R.D.Sun, H.Yoshiki, D.A.Tryk, K.Hashimoto, A.Fujishima; Electrochemistry, **67**, 11 **(1999)**.

[4] J.Springer, E.M.Ozsan, A.Kazandjian, N.Niegish, M.Mennig, H.Schimit, J.Feichtinger, M.Hartmann, L.De Rosa, F.Bellucci; EEC IV RTD Framework Publishable Report, **(1999)**.

[5] L.De Rosa, C.R.Tomachuk, J.Springer, D.B.Mitton, S.Saiello, F.Bellucci; Materials and Corrosion, **55**, 602 **(2004)**.

[6] C.R.Tomachuk, L.De Rose, J.Springer, D.B.Mitton, S.Saiello, F.Bellucci; Materials and Corrosion, **55**, 665 **(2004)**.

[7] C.R.Tomachuk, D.B.Mitton, J.Springer, T.Monetta, F.Bellucci; Materials and Corrosion, **57**, 394 **(2006)**.

[8] A.W.Czanderma, F.J.Pern; Solar Energy Materials and Solar Cells, **43**, 101 **(1996)**.

[9] Y.Xu, C.Yan, J.Ding, Y.Gao, C.Cao; Progress in Organic Coatings, **45**, 331 **(2002)**.

[10] P.Carbonini, T.Monetta, P.Mastronardi, F.Bellucci; Progress in Organic Coatings, **29**, 13 **(1996)**.

[11] M.Del Grosso Destreri, J.Vogelsang, L.Fedrizzi, F.Deflorian; Progress in Organic Coatings, **37**, 57 **(1999)**.

[12] P.L.Bonora, F.Deflorian, L.Fedrizzi; Electrochimica Acta, **41**, 1073 **(1996)**.

[13] G.W.Gilby; Ethylene vinyl acetate copolymers, in: Developments in rubber technologies-3. London Applied Science Publishers Ltd., **(1982)**.

[14] M.L.B.Martínez, T.P.F.Gómez, J.M.M.Martínez; Adhesives Age, **4**, 32 **(2001)**.

[15] M.Giurginca, L.Popa, T.Zaharescu; Polymer Degradation and Stability, **82**, 463 **(2003)**.

[16] N.S.Allen, M.Edge, M.Rodríguez, C.M.Liauw, E.Fontán; Polymer Degradation and Stability, **71**, 1 **(2001)**.

[17] J.A.R.Marcilla, J.A.R.Labarta, F.J.Sempere; Polymer, **42**, 5343 **(2001)**.

[18] I.C.McNeil, A.Jamieson, D.J.Toshand, J.J.McClune; European Polymer Journal, **12**, 305 **(1976)**.

[19] F.J.Pern, A.W.Czanderna; Solar Energy Materials and Solar Cells, **25**, 3 **(1992)**.

[20] F.J.Pern; Polymer Degradation and Stability, **41**, 125 **(1993)**.

[21] C.G.Roffey; Photopolymerization of Surface Coatings. New York, John Wiley & Sons, **(1982)**.

[22] A.G.Ghaffar, G.Scott; European Polymer Journal, **13**, 83 **(1977)**.

[23] A.G.Ghaffar, G.Scott; European Polymer Journal, **13**, 89 **(1977)**.

[24] R.Zhang, P.E.Mallon, H.Chen, C.M.Huang, J.Zhang, Y.Li, Y.Wu, T.C.Sandreczki, Y.C.Jean; Progress in Organic Coatings, **42**, 244 **(2001)**.

[25] R.P.Singh, N.S.Tomer, S.V.Bhadraiah; Polymer Degradation and Stability, **73**, 443 **(2001)**.

[26] M.Pulat, C.Senvar; Polymer Testing, **14**, 115 **(1995)**.

[27] A.Eisenberg, M.King; Ion-Containing Polymers-Physical Properties and Structure. New York, Academic Press, **(1977)**.

[28] Y.Lee, S.Han, M.H.Kwon, H.Lim, Y.S.Kim, H.Chum, J.S.Kim; Applied Surface Science, **203&204**, 875 **(2003)**.

[29] L.Holiday; Ionic Polymers. London, Applied Science Publishers Ltd., **(1975)**.

[30] A.Eisenberg, M.King; Introduction to Ionomers, New York, Wiley & Sons, **(1998)**.

[31] D.M.Brasher, A.H.Kingsbury; Journal of Applied Chemistry, **4**, 62 **(1954)**.

[32] C.I.Elsner, A.R.Di Sarli; Journal of the Brazilian Chemistry Society, **5**, 15 **(1994)**.

[33] E.E.Schwiderke, A.R.Di Sarli; Progress in Organic Coatings, **14**, 297 **(1987)**.

[34] H.Leidheiser Jr., M.W.H.Kendig; Corrosion, **32**, 69 **(1976)**.